mgr inż. Przemysław Palacz[1)*)]
ORCID: 0000-0002-2040-3494
dr hab. inż. Maciej Major, prof. PCz[1)]
ORCID: 0000-0001-5114-7932

Preliminary numerical analysis of the stiffness of non-standard assembly connections of steel I-beams

Wstępna analiza numeryczna sztywności niestandardowych połączeń montażowych stalowych belek dwuteowych

DOI: 10.15199/33.2024.04.01

Abstract. Connections are an indispensable element of every steel structure because they enable easy and quick assembly of prefabricated structural elements on the construction site. The article covers the initial analysis of non-standard connections of steel I-beams in relation to commonly used connections in steel building structures. An analysis of beams with connections was carried out and a finite element test was performed for two beam mounting schemes: cantilevered and simply supported. The parameters tested were stresses, strains and initial rotational stiffness of the connections. The results showed that two of the four proposed non-standard connections were characterized by high load transfer efficiency and greater rotational stiffness compared to standard connections.

Keywords: connections of steel structures; bolted connections; connecting steel I-beams; load-bearing capacity of connections; FEM analysis.

Streszczenie. Połączenia są nieodzownym elementem każdej konstrukcji stalowej, ponieważ umożliwiają łatwy i szybki montaż prefabrykowanych elementów konstrukcji na budowie. Artykuł obejmuje wstępną analizę niestandardowych połączeń stalowych belek dwuteowych w porównaniu z powszechnie stosowanymi w budowlanych konstrukcjach stalowych, a także badanie dwóch schematów zamocowania belki wspornikowej oraz swobodnie podpartej metodą elementów skończonych. Badanymi parametrami były naprężenia, odkształcenia oraz początkowa sztywność obrotowa połączeń. Wyniki wykazały, że dwa z czterech zaproponowanych niestandardowych połączeń charakteryzowały się dużą efektywnością przenoszenia obciążeń oraz większą sztywnością obrotową w porównaniu z połączeniami standardowymi.

Słowa kluczowe: połączenia konstrukcji stalowych; połączenia skręcane; łączenie stalowych belek dwuteowych; nośność połączeń; analiza MES.

Individual elements in each steel structure require connection. For this purpose, several types of connections are used: welded; twisted; riveted and glued [1]. Easy connection of structure elements during assembly on the construction site is possible thanks to screw connectors [2]. Bolted connections have many advantages, e.g. easy and quick assembly or disassembly of the structure, and at the same time enable the repair and replacement of damaged elements [1]. Connections in steel structures play a very important role because damage to the connection not only causes the redistribution of internal forces, but may also lead to structure failure [3]. Properly designed connections transfer the loads from individual structure elements to the load-bearing elements, ensuring its safe operation [4].

Many researchers analyze various design solutions for connections operating in various conditions. Zhihua Chen et al in paper [5] proposed an innovative modular connection design in steel structures with intermediate plug device and beam-beam bolt system as horizontal and vertical connections respectively. The connection design is designed to ensure easy installation, eliminating on-site welding. The authors performed two static uniaxial loading tests and four cyclic loading tests on the T-shaped joint to investigate its load-bearing capacity. The results showed that due to the two-piece connection structure, gaps develop between the upper and lower columns, which affect the deformation and stress distribution in the joint, and the weld quality of the joints is insufficient to ensure overall safety. In turn, Yanxia Zhang et al. in the article [6] proposed an innovative pole-to-pillar connection using self-tapping screws, which also eliminates welding on the construction site. The authors conducted experimental tests and tests using the finite element method, and proposed formulas for calculating the load-bearing capacity of a new type of connection based on the yield line theory. The results of the tests showed that the proposed connection using self-tapping screws is able to effectively connect elements while reducing implementation costs. Jianfen Li et al. in their work [7] presented an innovative form of prefabricated H-shaped connections of steel beams with steel pipes filled with concrete. They investigated the behavior of novel beam-to-column connections using cyclic load tests. The test results showed

[1)] Politechnika Częstochowska, Wydział Budownictwa
[*)] Correspondence address: przemyslaw.palacz@pcz.pl

that the proposed beam-column connections were characterized by high bending strength. Moreover, it was found that the thickness and yield strength of the steel column tube have a significant impact on the bending and deformation load-bearing capacity of the connection.

Experimental and numerical results show that the fatigue strength of joints can be influenced by many factors, such as the bolt pre-tension force, hole size and bolt arrangement [8]. Their load--bearing capacity is also influenced by the condition of the connection and weather conditions, which, for example, may favor corrosion. Shidong Nie et al. in the article [9] presented experimental tests of the load-bearing capacity of bolted connections made of high-strength steel subjected to corrosion. They performed corrosion tests initially on nine samples subjected to accelerated corrosion, and then examined the mechanical properties of these joints with different degrees of corrosion using static tensile tests. On this basis, they formulated a mathematical relationship between the mass loss rate and corrosion time and analyzed the mathematical relationships between the mass loss rate and mechanical indices, including slip ratio, bolt prestress, slip load, or failure load. Ultimately, they found that the corrosion environment had a significant impact on the slip load, slip coefficient and preload of bolts in bolted joints. In turn, Chao Jiang et al. in the article [10] presented parametric studies of the fatigue behavior of shear friction joints and proposed a procedure for predicting the fatigue life of steel friction joints using the finite element method and verified it with the results of fatigue tests. They found that the fatigue behavior of single shear plane connections is greatly influenced by the number of bolts, steel grade and hole making process, while the fatigue behavior of dual shear plane connections is largely influenced by bolt prestressing, slip coefficient, main plate thickness, steel grade and the process of making holes. The same authors in the article [11] examined the influence of corrosion on the fatigue properties of friction screw connections and showed, among others, that the fatigue life of friction connections may be significantly reduced by corrosion. If the mass loss rate of the joints exceeds 7.8%, the fatigue strength is less than 100 MPa, which does not meet the requirements of Eurocode 3.

Bolted connections are commonly used in steel structures, and the load--bearing capacity of bolted connections decreases at elevated temperatures [12]. In their works, many authors analyzed screw connections under elevated temperature conditions [13], [14], [15]. Weiyong Wang et al. in [13] showed that at elevated temperature, the sliding load decreases faster than the failure load, and the critical temperature from brittle failure to ductile failure is about 500 °C. Zhihao Chen et al. in the article [14] presented fire tests of end--plate made of high-strength steel. They investigated the mechanical properties at ambient temperature and fire resistance of end-plate joints with different endplate thicknesses and showed that endplate thickness had a large impact on increasing the joint stiffness at ambient temperature, while the critical temperature and fire resistance were not significantly improved when thicker endplate was used. In turn, the authors in article [15] tested the load-bearing capacity of class 8.8 bolts in natural fire conditions. They showed that the behavior of the bolts is not reversible when heated to 500°C and the load loss can be 40%, and the ductility of the bolts increases significantly when the peak cycle temperature is 800°C.

The analyzed connections are classified as flexible connections, which reduce the load-bearing capacity of structures. The rotational stiffness of the connection is influenced primarily by the geometry of the node elements together with the bolts and adjacent elements of the connected beams [16]. The authors in publication [17] presented an analysis of the tests carried out on end-plate joints and showed that all joints are deformable and their rotational stiffness and load-bearing capacity have different values. The authors showed that the difference in rotational stiffness is influenced by, among others, deformations of end plates. The flexibility of connections affects the load-bearing capacity and stability of the structure. The compliance of a node can be assessed from the relationship between the bending moment occurring in the connection and the angle of rotation of this connection, i.e. using the M-ϕ curve [17].

In this article, we present a preliminary analysis of non-standard steel I-beam connections compared to commonly used connections. The analysis of the proposed non-standard assembly contacts aims to develop a way to reduce the number of screw connectors in such a way that benefits resulting from faster implementation of the assembly process, which is ultimately to be carried out by the robot arm, can be obtained. Technological development and increasing requirements for new technologies determine the search for new design solutions, including connections that can be implemented using robot arms. Currently, we do not offer solutions that are intended to replace those that require human hands.

The process of building a structure can be divided into the implementation phase and the operation phase. In the implementation phase, the structure is assembled and acquires the assembly load-bearing capacity, while in the operation phase it must ensure safety resulting from the designed load--bearing capacity. By separating these individual stages, the process of erecting objects could be carried out by different devices, so in the first phase the structure elements would be assembled by screwing, and in the second by welding, obtaining the full designed load-bearing capacity and high stiffness. Therefore, the new technological solutions proposed in the article are an introduction to the discussion, thanks to which in the future they can be introduced into the construction industry, using dedicated robots in the assembly process. The analyzed connections were compared on the basis of stress distribution and initial rotational stiffness.

The aim and scope of work

The aim of the work was to check non-standard connections of steel I-beams in terms of effectiveness of use in structures. Their initial rotational stiffness was assessed in comparison to standard, commonly used assembly joints, using dedicated technological solutions, which, as a result of developing an appropriate connection standard, will increase the efficiency of the structure assembly process or its operation itself. The diagrams of the analyzed I-beam connections are shown in the Figure 1.

In order to perform a numerical analysis of the connections, two single--span static diagrams were considered, including a cantilever beam (Figure 2a) and a simply supported beam (Figure 2b), in which traditional bolted, end-plate and overlapping connections were introduced in the middle of their span (Figure 1a, b, c) and developed custom modified connections (Figure 1d, e, f, g).

An analysis was performed of 1.3 m long beams made of hot-rolled I-shaped IPE160 profile made of S235 steel. The cantilever beam was loaded with one concentrated force F_1 of 21.67 kN, which was applied at a distance of 1.2 m from its restraint (Figure 2a), while the simply supported beam was loaded with two forces F_2 of 65 kN each, which were applied at distances 0,4 m from each beam support (Figure 2b). The declared force values were accepted as permissible in the adopted diagrams using up to 95% of the ultimate limit state and serviceability of the beam cross-section.

Based on analytical calculations, the maximum internal forces were obtained and the load-bearing and serviceability limit state conditions were checked for the beam cross-section adopted on the basis of PN-EN 1993-1-1 [18]. The maximum deflections of the considered beams due to the adopted boundary conditions were read in the Ansys program (the model is described later in the article). Diagrams of internal forces and deflections of a continuous reference beam without a connection are shown in Figure 3.

The ultimate limit state conditions for bending and shear and the permissible deflections of the adopted beam were calculated in accordance with the standard [18]. The utilization of the cross-section in the ultimate limit state of both the cantilever beam and the simply supported beam in the case of the adopted static and load patterns was 89.38%. The permissible deflection was assumed to be L/250 for secondary beams in accordance with the standard [18]. The serviceability limit state condition for the cantilever beam was 92.03%, and for the simply supported beam it was 36.77%. In addition, standard beam connections were dimensioned (Figure 1a, b, c) in accordance with the standard [19]. The load-bearing conditions of the connections are presented in Table 1.

A preliminary assessment of the performance of commonly used steel structural connections, in the case of the adopted static schemes of I-beams, was made by comparing their vertical displacements with the displacements obtained as a result of the impact of the same type of loads on the reference beam, modeled as a continuous IPE 160 profile made of S235 steel. Then, the developed modified connections for steel I-beams were subjected to numerical tests. The structural diagrams of commonly used connections are shown in Figure 4, while the diagrams of modified connections are presented in Figure 5. The numerical analysis of all structural connections for steel I-beams was performed using the finite element method using the Ansys Research 2021 program (the model is described later in the article). The results obtained for the considered types of connections were compared with each other in relation to the values of stresses, displacements and initial rotational stiffness.

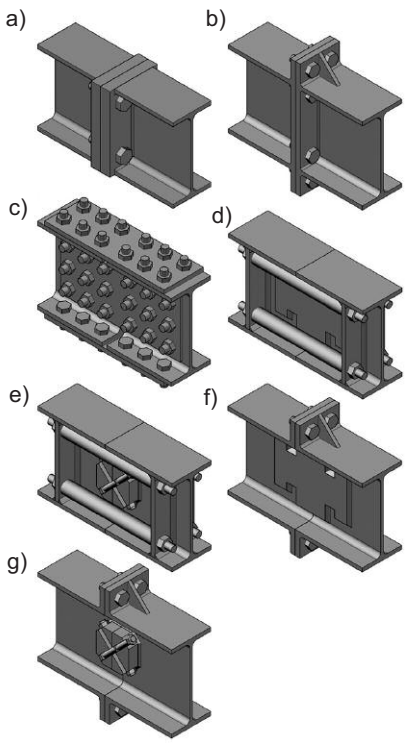

Fig. 1. Analyzed connections of steel I-beams: a) end-plate joint; b) end-plate joints with bolts extended beyond the cross-section; c) overlapping; d) partially welded with bolts inside the cross-section; f) with a cross-bolt on the web and bolts inside the cross-section; f) partially welded with bolts extending beyond the cross-section; g) with a cross bolt on the web and bolts extended beyond the cross--section

Rys. 1. Analizowane połączenia stalowych belek dwuteowych: a) doczołowe; b) doczołowe ze śrubami wysuniętymi poza przekrój; c) zakładkowe; d) częściowo spawane ze śrubami wewnątrz przekroju; e) ze śrubą krzyżową na środniku oraz śrubami wewnątrz przekroju; f) częściowo spawane ze śrubami wysuniętymi poza przekrój; g) ze śrubą krzyżową na środniku oraz śrubami wysuniętymi poza przekrój

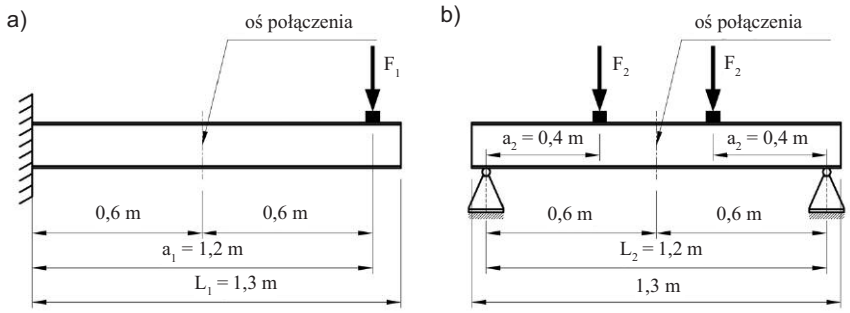

Fig. 2. Static diagrams of beam attachment: a) cantilever; b) simply supported beam

Rys. 2. Schematy statyczne zamocowania belki: a) wspornik; b) belka swobodnie podparta

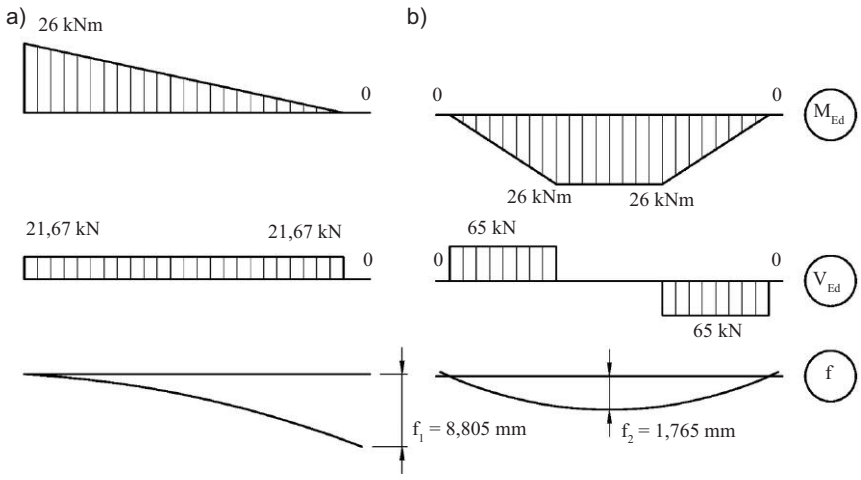

Fig. 3. Diagrams of bending moments – M_{Ed}, shear forces – V_{Ed} and deflections – f for the analyzed beam attachment: a) cantilever; b) simply supported
Rys. 3. Wykresy momentów zginających – M_{Ed}, sił tnących – V_{Ed} oraz ugięć – f w przypadku analizowanych schematów belek: a) wspornikowej; b) swobodnie podpartej

Table 1. Ultimate limit state conditions of the analyzed standard beam connections, shown in Fig. 1a, b, c
Tabela 1. Warunki stanu granicznego nośności analizowanych standardowych połączeń belek, przedstawionych na rysunku 1a, b, c

Connection type	Load capacity condition for a cantilever beam [%]	Load capacity condition for a simply supported beam [%]
a) end-plate	47.90	95.70
b) end-plate joints with screws extended beyond the cross-section	49.00	98.00
c) overlapping	46.64	93.28

In a partially welded connection with bolts inside the cross-section (Figure 5a), the assembly joint is achieved by mutual pressure between the I-beam sections and the welded sheet on both sides of the web, e.g. by laser welding, which is intended to position the assembled elements and ensure connection during the implementation phase. The shape of the sheet was adopted due to the increase in the length of the weld. The connection is then prestressed with bolts passing through the ribs and the sleeves between them, thus ensuring load-bearing capacity during the operational phase. In turn, in combination with the cross bolt on the web (Figure 5b), the assembly joint is achieved by mutual pressure of the I-beam sections and by a twisted cross connector in order to position the assembled elements and ensure connection during the implementation phase. Then the connection is prestressed using bolts passing through the ribs and sleeves between them, analogously to the first one. In partially welded connections (Figure 5c) and with a cross bolt (Figure 5d), the assembly connection is carried out analogously to the previous connections (Figures 5a and b), while the operational load-bearing capacity is obtained by prestressing the bolts extended beyond the cross-section of the connected beams. The presented studies constitute an introduction to the analysis of complex assembly joints. Ultimately, individual solutions in the implementation and operation phases can be replaced with alternative, innovative solutions enabling the assembly of structures by dedicated machines, i.e. without the use of human hands.

Numerical model

Numerical models of all connections were made in the Ansys Research 2021 program by declaring geometry, boundary conditions and loads identical to the analytical calculations. In order to maintain the symmetry of the system in a simply supported beam, non-sliding supports were adopted on both sides of the beam to determine the rotational stiffness of the connections. In both cases, it was assumed that the beams were protected against buckling by blocking the belts from moving horizontally. Examples of numerical models of one of the analyzed connections are shown in Figures 6 and 7.

For steel profiles and connection elements, 3D SOLID finite elements with an adaptive mesh size, but not larger than 0.005 m, were used. The bolts in the connections were modeled from three elements: two nuts and a pin (Figure 8). BONDED contact is used between the nuts and the rod. The values of the initial prestressing forces in the bolts were adopted in accordance with the standard [20], assuming the nominal values of the required prestressing forces Fp,C. In the case of M12 screws, class 10.9, a prestressing force of 59 kN was assumed, while in the case of M16 screws, class 10.9, a prestressing force of 110 kN was assumed. On the contact surfaces, the contacts between the connection elements were assumed to be frictional, while the value of the friction coefficient between the elements was assumed to be $\mu = 0.2$. The linear-elastic material properties of the beam and connection elements made of S235 steel were adopted on the basis of the standard [18], while in the case of class 10.9 bolts they were adopted on the basis of the standard [19]. Due to the preliminary comparative analysis of various types of assembly connections, a type of static linear analysis was adopted. Numerical calculations were made in two time steps, the first step included the initial prestressing force of the bolts, while in the second step external loads were added.

Discussion of the numerical analysis

In the analyzed models, stresses and displacements were taken into account. The distribution of longitudinal normal stresses (along the X axis) in the case of one of the connection variants is shown in Figure 9.

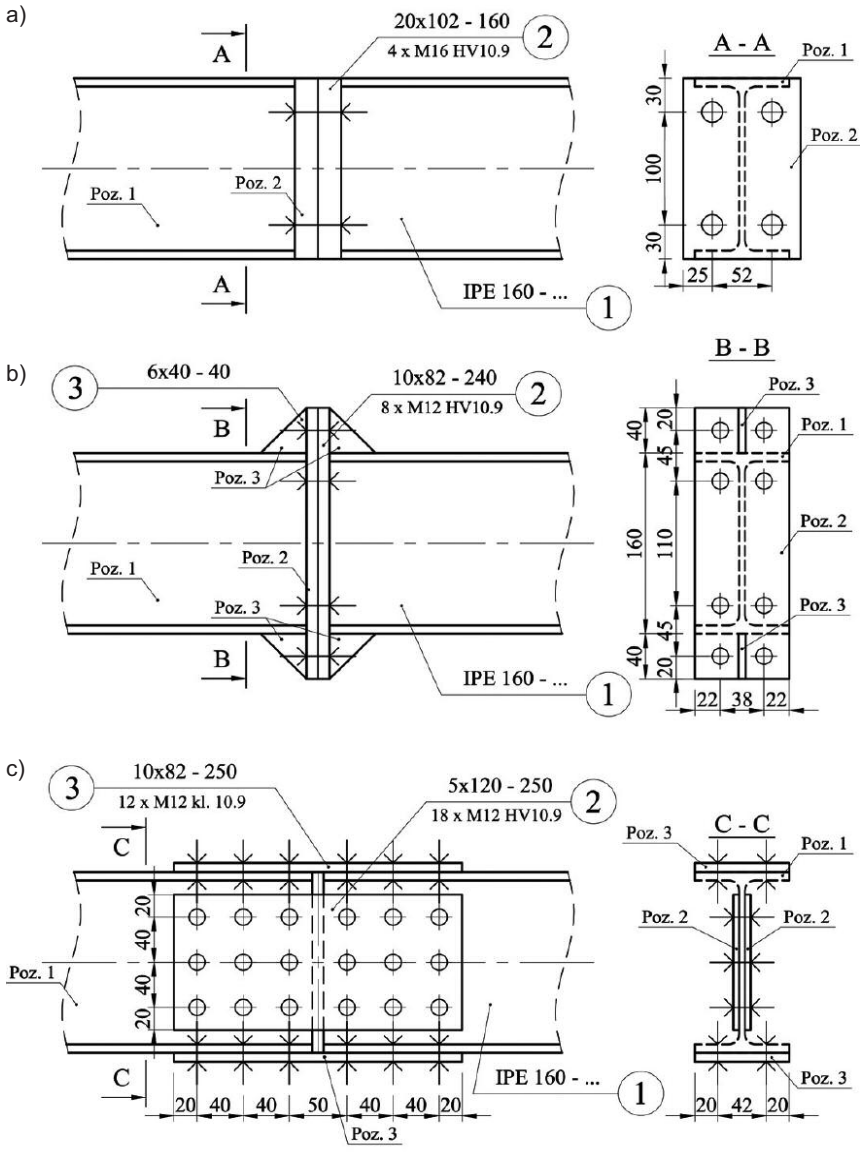

Fig. 4. Construction diagrams of commonly used connections for steel I-beams [mm]: a) end-plate joint; b) end-plate joints with bolts extended beyond the cross-section; c) overlapping

Rys. 4. Schematy konstrukcyjne powszechnie stosowanych połączeń stalowych belek dwuteowych [mm]: a) doczołowe; b) doczołowe ze śrubami wysuniętymi poza przekrój; c) zakładkowe

The distribution of normal stresses (along the X axis) in the cantilever (Figure 9a) shows that in the steel beam, tensile stresses predominate mainly in the upper section of the section near the restraint, i.e. in the place of the highest bending moment (stresses do not exceed 235 MPa). Moreover, the stress distribution in a simply supported beam (Figure 9b) shows that in a steel beam, compressive stresses also predominate in the upper section band in the middle of the beam span, i.e. at the place of the highest bending moment. These stresses also do not exceed 235 MPa, which proves compliance with the analytical calculations of the cross-section's load--bearing capacity. A summary of the distribution of reduced stresses in all analyzed connections is shown in Figure 10. This summary concerns an unfavorable scheme, i.e. a simply supported beam, because the maximum bending moment occurs in the joint axis.

By analyzing the distribution of stresses in the connections (Figure 10), the efficiency of the connections can be assessed. In the end-plate connection (Figure 10a), the stresses in the end plate near the screws in the tension zone are clearly visible, but the total stresses do not exceed the permissible ones. In a end-plate connection with bolts extended outside the cross-section (Figure 10b), forces are transferred much more effectively through the connectors and the end plate than in the connection with bolts inside the cross-section, despite the thinner end plate and smaller diameter of the bolts. In aoverlapping joint (Figure 10c), the stresses are evenly distributed in the overlaps in both the flanges and the web. In modified connections with bolts located inside the cross-section (Figure 10d and 10e), increased stresses occur at the contact between the ribs and the sleeves in the tension zone, while by using a welded overlay to the web (Figure 10d), it was possible to reduce the thickness of the ribs and the diameter of the bolts. The cross bolt (Figure 10e) is located mainly in the neutral axis of the cross-section, so it transfers smaller forces, resulting in higher stresses in the ribs and sleeves in the tension zone in relation to the connection with the cap welded to the web (Figure 10d). In modified connections with bolts located outside the cross-section (Figures 10f and 10g), bolted connectors extended outside the cross-section transfer forces more effectively, while the cap welded to the web (Figure 10f) effectively transfers forces from the web. Increased stresses appear in the tension zone where the cover plate meets the web. The cross bolt (Figure 10g), similarly to the connection (Figure 10e), transmits smaller forces, which is why there are greater stresses in the front connectors. Despite increased stresses in some places at the joint joints, they do not exceed 235 MPa. The presented connections therefore allow you to effectively connect beams within the yield strength of steel. Attention should be paid to the high stresses in the screws themselves, because they are made of a material with a different yield strength, which is 900 MPa, while the stress maps in Figure 10 cover the range up to 235 MPa. The distribution of stresses

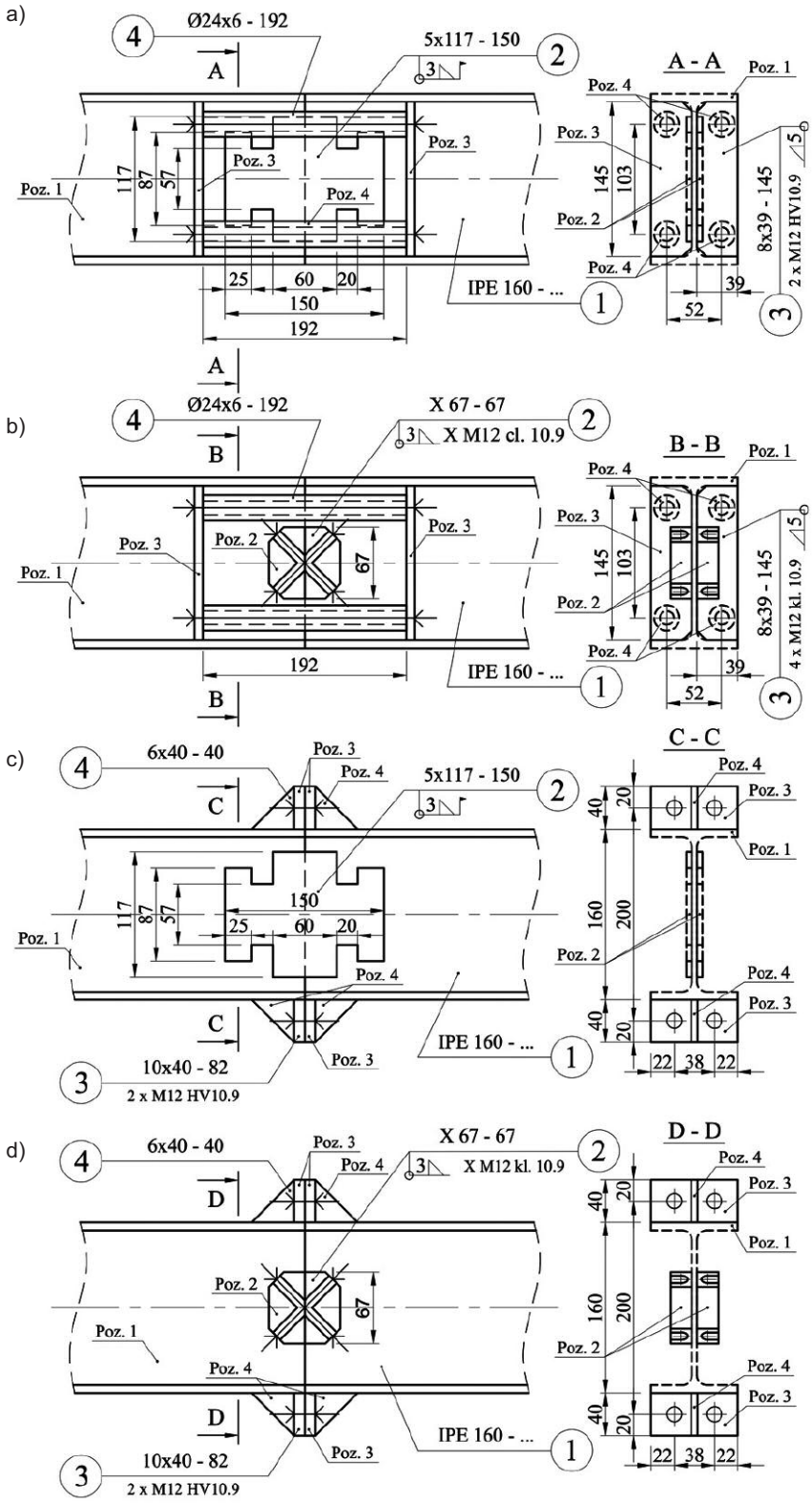

Fig. 5. Diagrams of the developed modified connections [mm]: a) partially welded with bolts inside the cross-section; b) with a cross-bolt on the web and bolts inside the cross--section; c) partially welded with bolts extending beyond the cross-section; d) with a cross--bolt on the web and bolts extended beyond the cross-section

Rys. 5. Schematy opracowanych połączeń zmodyfikowanych [mm]: a) częściowo spawane ze śrubami wewnątrz przekroju; b) ze śrubą krzyżową na środniku oraz śrubami wewnątrz przekroju; c) częściowo spawane ze śrubami wysuniętymi poza przekrój; d) ze śrubą krzyżową na środniku oraz śrubami wysuniętymi poza przekrój

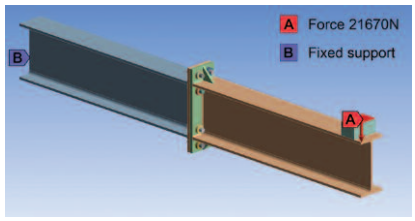

Fig. 6. Numerical model of one of the analyzed variants of the cantilever beam with the marked force and boundary conditions

Rys. 6. Model numeryczny jednego z analizowanych wariantów belki wspornikowej z zaznaczonymi siłami oraz warunkami brzegowymi

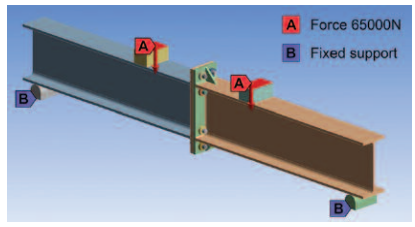

Fig. 7. Numerical model of one of the analyzed variants of a simply supported beam with marked forces and boundary conditions

Rys. 7. Model numeryczny jednego z analizowanych wariantów belki swobodnie podpartej z zaznaczonymi siłami oraz warunkami brzegowymi

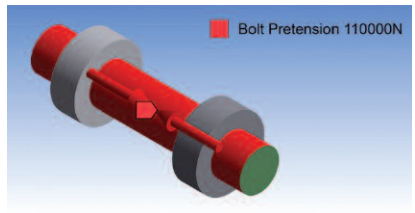

Fig. 8. Numerical model of the bolt with the indicated pretension force

Rys. 8. Model numeryczny śruby ze wskazaną siłą wstępnego sprężenia

in the bolts is shown in Figure 11. They do not exceed 700 MPa, which proves compliance with the analytical calculations of the bolt load capacity.

Figure 12a shows that the largest displacement occurs at the end of the cantilever span, while Figure 12b shows that it occurs in the middle of the span at the connection point. The displacement of a connected beam can only be determined using a numerical model, because the standard [17] does not specify a method for calculating the displacements of beams with connections. A summary of the maximum displacements for all analyzed connections is presented in Table 2.

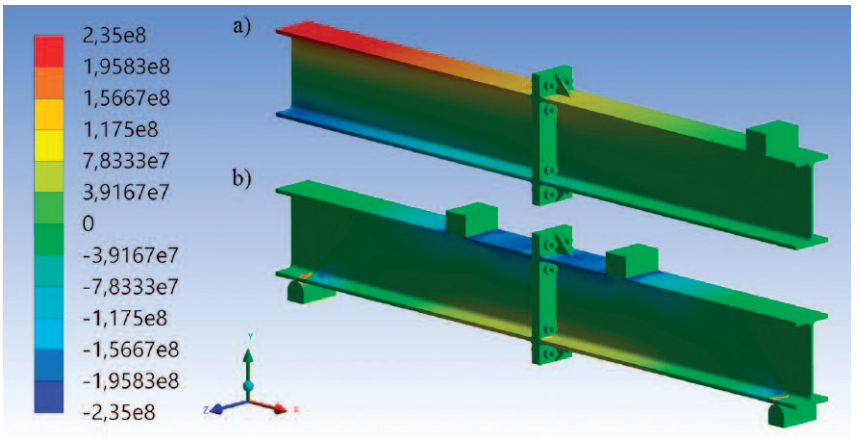

Fig. 9. Distribution of normal longitudinal stresses for the analyzed model of a end-plate connection with bolts extended beyond the cross-section (Pa): a) cantilever beam; b) simply supported beam

Rys. 9. Rozkład naprężeń normalnych podłużnych w przypadku analizowanego modelu połączenia doczołowego ze śrubami wysuniętymi poza przekrój (Pa): a) belka wspornikowa; b) belka swobodnie podparta

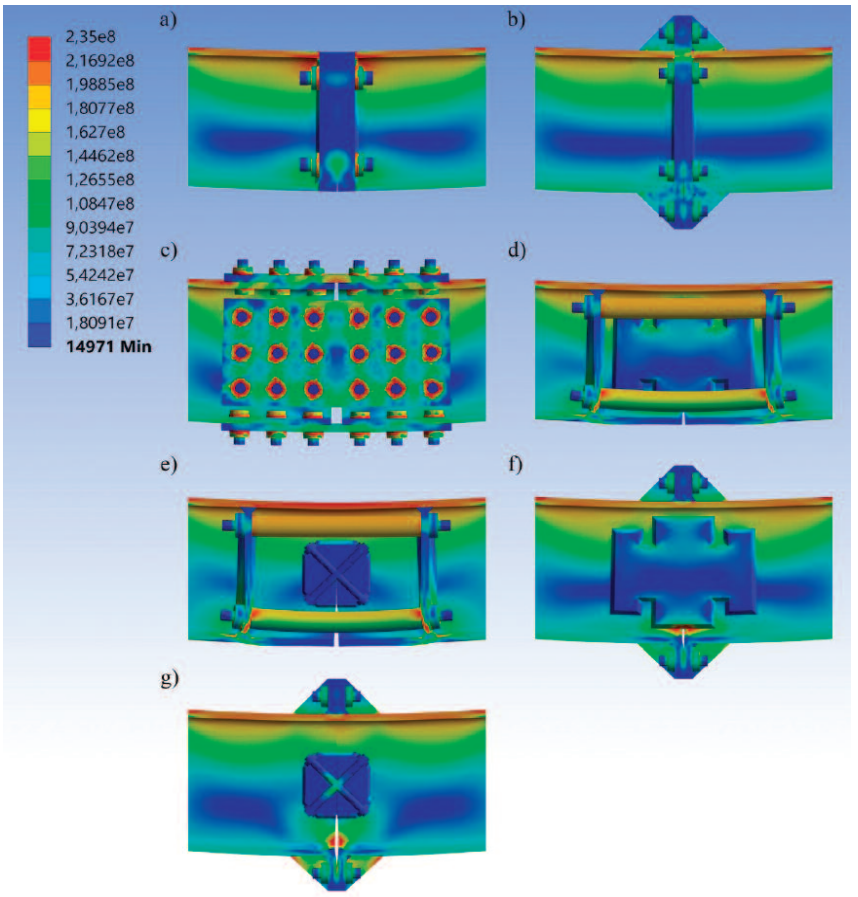

Fig. 10. Stress distribution in the analyzed connections for a simply supported beam [Pa], as shown in Fig. 1. Deformations shown at 35x magnification – description in text

Rys. 10. Rozkład naprężeń w analizowanych połączeniach w przypadku belki swobodnie podpartej [Pa], zgodnie z rysunkiem 1. Deformacje pokazane w 35-krotnym powiększeniu – opis w artykule

Analyzing the maximum deflections of the cantilever beam presented in Table 2, it can be seen that the connection ensuring the smallest vertical displacement is the end-plate connection with bolts extended outside the cross-section (Figure 10b), because the displacement is 9.079 mm, which is closest to the maximum deflection of the cantilever beam without the connection, for which the deflection is equal to 8.835 mm. The next comparable connections are: partially welded with bolts inside the cross-section (Figure 10d) with a vertical displacement of 9.114 mm; overlapping (Figure 10c) with a displacement of 9.126 mm; end-plate connection with bolts in side the cross-section (Figure 10a) with a displacement of 9.140 mm and a partially welded connection with bolts extended outside the cross-section (Figure 10f) with a displacement of 9.198 mm. Due to the exceeded permissible deflections, the connections with cross-head screws were the worst (Figure 10e and 10g) with displacements of 9.760 mm and 9.912 mm, respectively.

Analyzing the maximum deflections of the simply supported beam with the analyzed connections, it was shown that the smallest deflections are provided by a partially welded connection with bolts extending beyond the cross-section (Figure 10f) and a end-plate connection with bolts extending beyond the cross-section (Figure 10b). These connections provide deflections of 1.840 mm and 1.843 mm, respectively, which are closest to the maximum deflection of a simply supported beam without a connection with a deflection of 1.765 mm. The end-plate connections (Figure 10a) and the partially welded connection with screws inside the cross-section (Figure 10d) are slightly worse, with deflections of 1.893 mm and 1.962 mm, respectively. The worst-performing connections in terms of vertical displacements are the connections with cross bolts (Figures 10e and 10g) and the overlapping joint (Figure 10c) with displacements of 2.045 mm, 2.077 mm and 2.032 mm, respectively. Despite obtaining larger displacements, all connections meet the condition of permissible deflection in the case of a simply supported beam. It indicates the effectiveness of their work in terms of vertical displacements in the analyzed static diagrams of steel I-beams.

Moreover, based on the read displacements, their difference was calculated in the case of beams without

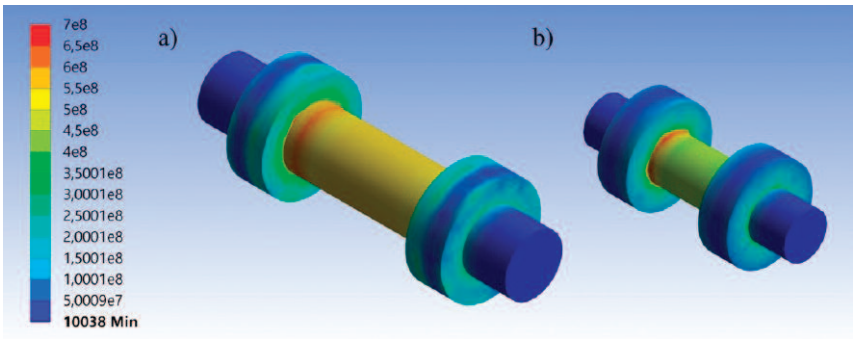

Fig. 11. Distribution of reduced stresses in numerical models of bolts [Pa]: a) M16 bolt; b) M12 bolt

Rys. 11. Rozkład naprężeń zredukowanych w modelach numerycznych śrub [Pa]: a) śruba M16; b) śruba M12

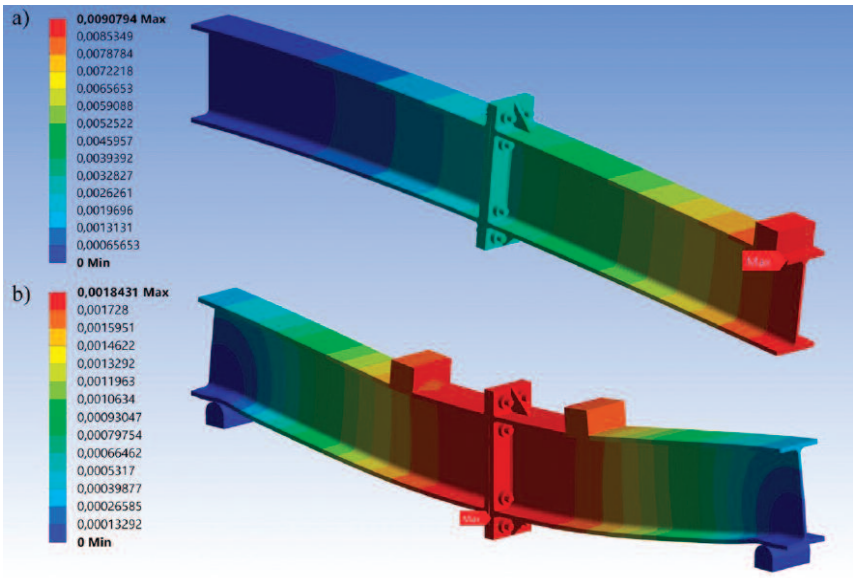

Fig. 12. Displacement maps for the analyzed model of the end-plate joint with bolts extended beyond the cross-section, deformations shown at 35x magnification [m]: a) cantilever beam; b) simply supported beam

Rys. 12. Mapy przemieszczeń w przypadku analizowanego modelu połączenia doczołowego ze śrubami wysuniętymi poza przekrój, deformacje pokazane w 35-krotnym powiększeniu [m]: a) belka wspornikowa; b) belka swobodnie podparta

Table 2. Maximum deflection in a cantilevered beam and a simply supported beam for the analyzed schemes of beam connections, shown in the same way as in Fig. 1

Tabela 2. Maksymalne ugięcie w belce wspornikowej oraz swobodnie podpartej w przypadku analizowanych schematów połączenia belek, pokazanych na rysunku 1

Analyzed connection model	Deflections for a	
	cantilever beam [mm]	simply supported beam [mm]
a.	9.140	1.893
b.	9.079	1.843
c.	9.126	2.032
d.	9.114	1.962
e.	9.760	2.045
f.	9.198	1.840
g.	9.912	2.077

and with connections, and then, using trigonometric relationships, the angles of rotation in the connections, resulting from the work of the connections themselves, were determined. An analysis of the initial rotational stiffness was also carried out in the case of bending moments in the linear-elastic range of 0 – 19 kNm, i.e. approximately $2/3M_{pl,Rd}$ of the beam's bending capacity. The deflections were also read for intermediate values of bending moments with a step of 3 kNm. The calculated values of the initial stiffness of the rotary joints are shown in Figure 13.

Analyzing the calculated initial rotational stiffness of the connections, it

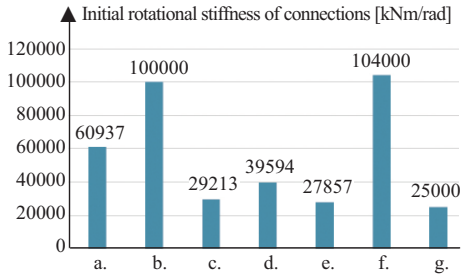

Fig. 13. Graph of the initial rotational stiffness of the connections, as shown in Fig. 1

Rys. 13. Początkowa sztywność obrotowa połączeń, zgodnie z rysunkiem 1

was found that the stiffest are the partially welded connection with bolts extending beyond the cross-section (Figure 10f) and the standard end-plate joint with bolts extending beyond the cross-section (Figure 10b). These connections provide initial rotational stiffness of 104,000 kNm/rad and 100,000 kNm/rad, respectively. Lower rotational stiffness is characteristic of the end-plate connection (Figure 10a) and the partially welded connection with bolts inside the cross-section (Figure 10d) with joint stiffness of 60937 kNm/rad and 39594 kNm/rad, respectively. The least stiff connections were the connections with cross bolts (Figures 10g and 10e) and the overlapping joint (Figure 10c) with stiffnesses of 25,000, 27,857 and 29,213 kNm/rad, respectively. The relationship diagrams between the bending moment in the connection and its angle of rotation (M-ϕ curves) are shown in Figure 14. A completely rigid node is characterized by the ordinate axis 0-M, while a perfectly articulated node is characterized by the 0-ϕ axis,

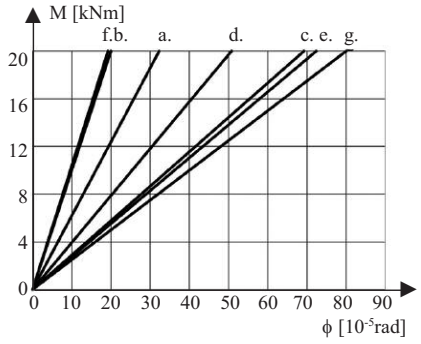

Fig. 14. Graph of the initial rotational stiffness of the analyzed joints, as shown in Fig. 1

Rys. 14. Wykres początkowej sztywności obrotowej analizowanych połączeń, pokazanych zgodnie z rysunkiem 1

so the straight M-ϕ is closer to the 0-M axis, the connection has greater rotational stiffness. As can be seen in Figure 14, the rotation angle of the connections calculated numerically increases linearly depending on the increasing bending moment, while experimental studies show that the characteristics of most nodes are curvilinear throughout the entire range of tests [17], this is related to the adopted linear-elastic in this work. Taking into account the assessment of the susceptibility of connections, as a result of the numerical analysis, it is possible to compare connections and evaluate them in terms of initial rotational stiffness.

Conclusions

As a result of the preliminary numerical analysis, the effectiveness of beam connections in terms of stresses and displacements was assessed. The best among the analyzed connections were the partially welded connection with bolts extending beyond the cross-section (Figure 1f) and the end-plate joint with bolts extending beyond the cross-section (Figure 1b). These connections are characterized by stresses not exceeding the permissible stresses for the adopted S235 steel and the highest initial rotational stiffness. However, it should be noted that in a prestressed end-plate connection with a full end plate (Figure 1b), appropriate flatness of the end plate surfaces is required, because unevenness created during welding the plate to the beam may prevent proper tensioning of the bolts. Moreover, in deformed contacts, uneven distribution of forces in the screws may occur, which may lead to their breakage. Additionally, these connections contain elements protruding beyond the cross-section, which in many cases is impossible to use in the structure. Another interesting connection is a partially welded connection with bolts inside the cross-section (Figure 1d), which also allows for effective connection of beams, while being a connection closed within the outline of the connected cross-section. The weakest connection variants turned out to be connections with cross bolts (Figures 1e and 1g), in which the permissible deflections for the cantilever beam were exceeded. However, it should be noted that high stiffness is not always desirable. The type of connection adopted therefore depends on the type of structure.

The results obtained for the numerical analysis of modified connections of steel I-beams showed that they may be an interesting alternative for use in connections of steel structure beams. Moreover, the analysis showed that there are alternative construction solutions to traditional ones that will effectively transfer the loads resulting from the operation of the structure. In the next stage of the research, the authors will pay attention to the efficiency of the developed connections of steel I-beams as a result of dynamic loads and will technologically improve the proposed solutions.

Literature

[1] Kontoleon MJ, Kaziolas DN, Zygomalas MD, Baniotopoulos CC. Analysis of steel bolted connections by means of a nonsmooth optimization procedure, Computers & Structures. 2003; ISSN 0045-7949, https://doi. org/10.1016/S0045--7949 (03) 00311-0.

[2] Palacz P, Major I. Strengthening the existing connection of steel beams with a column, MATEC Web Conference. 2020; https://doi. org/10.1051/matecconf/202031300032.

[3] Chen P, Gao F, Wan J. Experimental and numerical study of the tensile behavior of high--strength steel T-stub, Progress in Steel Building Structures. 2022; 24 (5): 40–50, 112. (in Chinese).

[4] Kozłowski A. Konstrukcje stalowe, Przykłady obliczeń według PN-EN 1993-1, Oficyna Wydawnicza Politechniki Rzeszowskiej, Rzeszów, 2010.(in polish).

[5] Zhihua Chen, Jiadi Liu, Yujie Yu, Chenhua Zhou, Rengjing Yan, Experimental study of an innovative modular steel building connection, Journal of Constructional Steel Research, Volume 139, 2017, Pages 69-82, ISSN 0143-974X, https://doi. org/10.1016/j. jcsr. 2017.09.008.

[6] Yanxia Zhang, Zheng Yang, Yanglong Li, Xiaotian Cheng, Zhewen Huang, Experimental and theoretical investigation of self-tapping bolt core tube flange column connection of prefabricated steel structure, Engineering Structures, Volume 278, 2023, 115482, ISSN 0141-0296, https://doi.org/10.1016/j.engstruct. 2022.115482.

[7] Jianfen Li, Ben Mou, Zian Wang, Cyclic behavior of column-to-column connections in novel prefabricated H-shaped steel beam to CFST column joint, Journal of Constructional Steel Research, Volume 200, 2023, 107657, ISSN 0143-974X, https://doi.org/101016/j. jcsr. 2022.107657.

[8] Puthli R, Fleischer O. Investigations on bolted connections for high strength steel members, Journal of Constructional Steel Research. 2001; ISSN 0143-974X, https://doi. org/10.1016/S0143-974X (00) 00017-1.

[9] Shidong Nie, Hui Wang, Bo Yang, Zhenghang Cheng, Xiyu Ye, Zhenye Chen, Corrosion-induced mechanical properties of shear bolted connections in high strength weathering steel. Thin-Walled Structures. 2023; ISSN 0263-8231, https://doi.org/10.1016/j. tws.2023.111013.

[10] Chao Jiang, Wen Xiong, C. S. Cai, Xiaoyi Zhou, Yichen Zhu, Yanjie Zhu, Parametric study on fatigue behavior of steel friction connections in shear, Journal of Constructional Steel Research, Volume 207, 2023, 107951, ISSN 0143-974X, https://doi.org/10.1016/j. jcsr.2023.107951.

[11] Chao Jiang, Wen Xiong, C. S. Cai, Xiaoyi Zhou, Yanjie Zhu, Corrosion effects on the fatigue performance of high-strength bolted friction connections, International Journal of Fatigue, Volume 168, 2023, 107392, ISSN 0142-1123, https://doi. org/10.1016/j. ijfatigue. 2022.107392.

[12] Lu Yonggui, You Yang, Zhang Wenchao, Song Jie, Wang Peijun, A Design Method for Thread-Fixed One-Side Bolted T-stub Connections at High Temperatures, Progress in Steel Building Structures, 23 (9), pp. 54 – 60, 2021. DOI: 10.13969/j. cnki. cn31-1893.2021.09.007.

[13] Weiyong Wang, Haojie Fang, Linbo Zhang, Experimental and numerical studies on the behavior of high strength steel shear connections at elevated temperatures, Fire Safety Journal, Volume 139, 2023, 103820, ISSN 0379-7112, https://doi.org/10.1016/j.firesaf. 2023.103820.

[14] Zhihao Chen, Weiyong Wang, Zhiruoyu Wang, Experimental study on high-strength Q460 steel extended end-plate connections at elevated temperatures, Journal of Constructional Steel Research, Volume 200, 2023, 107686, ISSN 0143-974X, https://doi.org/10.1016/j.jcsr.2022.107686.

[15] Hanus F, Zilli G, Fransse J-M. Behaviour of Grade 8.8 bolts under natural fire conditions – Tests and model, Journal of Constructional Steel Research. 2011; ISSN 0143-974X, https://doi. org/10.1016/j. jcsr. 2011.03.012.

[16] Basiński W. Wyznaczanie sztywności obrotowej doczołowych połączeń podatnych w metalowych konstrukcjach prętowych na podstawie pomiaru drgań, Rozprawa doktorska. Wydział Budownictwa Politechniki Śląskiej. Gliwice. 2006.

[17] Bródka J, Kozłowski A. Sztywność i nośność węzłów podatnych. Oficyna Wydawnicza Politechniki Rzeszowskiej. Białystok, Rzeszów. 1996.

[18] PN-EN 1993-1-1. Eurokod 3: Projektowanie konstrukcji stalowych – Część 1-1: Reguły ogólne i reguły dla budynków. 2006.

[19] PN-EN 1993-1-8. Eurokod 3: Projektowanie konstrukcji stalowych – Cześć 1-8: Projektowanie węzłów. 2006.

[20] PN-EN 1090-2. Wykonanie konstrukcji stalowych i aluminiowych – Część 2: Wymagania techniczne dotyczące konstrukcji stalowych. 2018.

Accepted for publication: 27.03.2024 r.